J Mater Sci (2010) 45:3974–3980
DOI 10.1007/s10853-010-4464-x

Drying of aerogel-bonded sands

Michael Reuß · Lorenz Ratke

Received: 13 November 2009 / Accepted: 2 April 2010 / Published online: 13 April 2010

Abstract The drying of foundry sands bonded by polymeric aerogels is of essential importance for their industrial application and of general interest in the context of drying theories for porous media, since in these new materials the interstices between the sand grains are partially filled with an open porous nanostructured material, the aerogel. We describe measurements on the drying of various foundry sands with different amounts of aerogelic binder made from resorcinol and formaldehyde in which we also varied the drying temperature. The results suggest that the nanostructured aerogel dictates completely the drying behaviour. Sand type and sand grain size are of minor relevance. A simple qualitative picture is developed describing the observations.

Introduction

In recent years, polymeric aerogels were developed as a new, nanostructured material with possible applications like binding material for sand cores and moulds in the foundry industry [1, 2]. As mould materials, they are very interesting especially for light alloy casting, because they ease the knock out cores, lead to castings with shiny surfaces, have decomposition products being almost pure carbon dioxide and water, allow to produce thin and complex cores and have the ability to uptake casting gases due to their high specific surface area [3–6].

Aerogels are nanostructured materials, containing up to 99 wt% air. They are manufactured by a sol–gel process [7–9]. After formation of a 3D network of colloidal particles, the wet gel has to be dried without shrinkage to avoid destruction of the network by stress gradients induced by capillary forces. The drying process can be supercritical or subcritical, depending in the case of resorcinol–formaldehyde (RF) aerogels [10] on the ratio between formaldehyde and catalyst used to initiate the formation of colloidal particles. In recent years, it was possible to synthesize RF aerogels by subcritical drying and thereby opening the field of possible applications [11]. These RF aerogels are typically catalyzed with weak bases like sodium carbonate. They have pore sizes from 10 nm to 1 μm. Their manufacturing process and their mechanical, chemical and physical properties are well described in the literature [8, 10–12].

For the foundry industry it is very important to avoid humidity in mould materials as good as possible because humidity has negative effects on castings being one of the origin of blowholes and ruptures [13, 14]. Usually sand mould materials contain a small amount of a binding material, like phenolic or urea formaldehyde resins, furans, epoxides and others [15]. The binder amounts are varied in foundries typically between 1 and 3 wt% with reference to the sand weight. All mould and cores contain, depending on the processing and the resin used, humidity and can adsorb and absorb water during storage. Since aerogelic binders start even with water solution containing colloidal particles and the wet gel containing up to 75 wt% water, this has to be removed completely before usage in foundry shops. Therefore, it is important to get a fundamental understanding of the drying process in foundry sands bonded by polymeric aerogels in order to optimize this kind of mould material. It also is of principal interest in the

M. Reuß · L. Ratke (✉)
Deutsches Zentrum für Luft- und Raumfahrt (DLR), Institut für Materialphysik im Weltraum, 51170 Köln, Germany
e-mail: lorenz.ratke@dlr.de

M. Reuß
e-mail: michael.reuss2@web.de

context of drying processes observed in porous materials [16–22], since in the case considered here the interstices in the more or less loosely packed sand is filled by a nanoporous material, the aerogel. Depending on the binder amount, the filling varies from almost zero to almost a hundred percent. We therefore describe in this paper experimental results on the drying of sands of different composition and provenience bonded by RF aerogels by measuring the density loss during isothermal anneals. We compare the experimental observations with models described in the literature [16, 18, 20, 21].

Experimental

We observed in the past years that moulds and cores prepared from mixtures of RF aerogels and sands never showed radial shrinkage. If moulded in a cylindrical tube of glass, polystyrol or polypropylene samples never developed even a small slit to the container during the drying process [1–5]. Therefore, filling of a sand–RF-aerogel mixture in a container and heating it to a certain temperature would induce a drying process in which all humidity being in the solution and generated as a result of the polycondensation reaction would have to leave the sample at the front face. Therefore, the drying process in our samples is quasi one dimensional and should ease a theoretical description.

We used different kinds of sand with different average grain sizes $\langle d \rangle$. An overview is given in Table 1.

We use three mullite type sands known as Cerabeads^{TM}, pure Silicon dioxide sand from Quarzwerke Frechen and pure aluminium oxide with the brand name Alodur®. The cylindrical containers with the samples were filled with the sand-binder mixture (5, 10, 15 and 20 wt% binder) to different heights. The diameter of all samples was 33 mm, the length of the samples was varied from 1.3 up to 55 mm. The binding solution was an aqueous solution of resorcinol ($C_6H_6O_2$, >99.0 wt%, Merck), formaldehyde (CH_2O, 37.7 wt%, Merck) and sodium carbonate (Na_2CO_3, 99.9 wt%, Merck) as catalyst after a special recipe developed in our institute [1–5].

Table 1 Sand types and their grain size used

Designation	Material	Average grain size (µm)	Vendor
Cerabeads 400	$3Al_2O_3\ 2SiO_2$	306	Hüttenes-Albertus
Cerabeads 650	$3Al_2O_3\ 2SiO_2$	173	Hüttenes-Albertus
Cerabeads 1450	$3Al_2O_3\ 2SiO_2$	100	Hüttenes-Albertus
Quartzsand 1	SiO_2	290	Quarzwerek Frechen
Sepasil 344-502	SiO_2	55	Quarzwerke Frechen
Alodur F80	Al_2O_3	181	Munk + Schmitz
Alodur F220	Al_2O_3	60	Munk + Schmitz

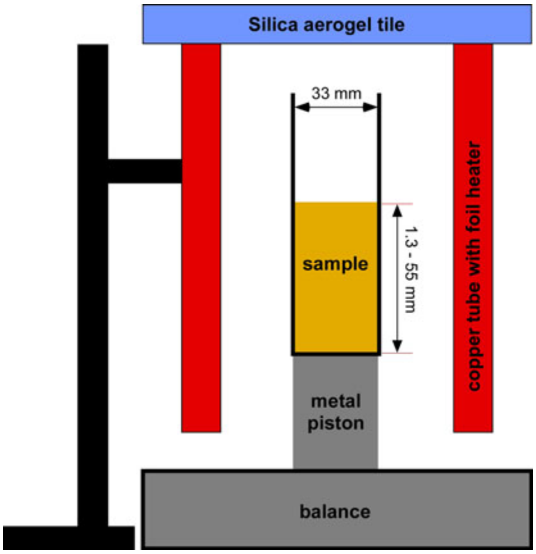

Fig. 1 Simple measurement set-up for recording the weight loss of aerogel-bonded sands at constant temperature

The sample was placed in a simple tube-like furnace shown in Fig. 1. This was built form a copper cylinder on which a heating foil was glued. The temperature in the tube was controlled by a thermocouple close to the sample. The top of the copper heater was closed with a lid of silica aerogel from Airglass^{TM}, Sweden, to avoid a chimney effect. The loss of mass during the drying process was recorded continuously by an electronic scale, which was connected to a computer. It was a scale of the type Scout II from Ohaus with an accuracy and a resolution of 0.01 g. Every 60 s a value was read out and stored in an Excel file. The relative mass loss was calculated from the mass at a given time t, $m(t)$, the initial $m(0)$ and the final mass after it was completely dry $m(t = \infty) = m_{end}$ as

$$\frac{\Delta m(t)}{\Delta m_{end}} = \frac{m(t) - m_{end}}{m(0) - m_{end}} \tag{1}$$

The microstructure of some samples was examined in a scanning electron microscope (SEM) using secondary electrons.

Results

A typical drying curve of an aerogel–sand mixture is shown in Fig. 2. The relative mass loss is shown as a function of drying time for the Quartzsand 1 sand (drying at 40 °C; only a few data points are shown). There is a short incubation period of a about 10 min before a measurable mass loss starts, which is shown in the insert. This

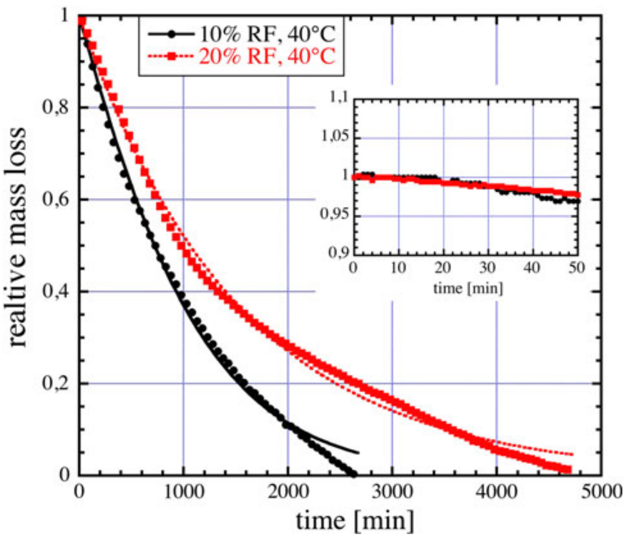

Fig. 2 Relative mass loss against time at 40 °C for the Quartzsand 1 sand (not all data points are shown). There is a short incubation period of a about 10 min (see *inset*) before a measurable mass loss starts followed by an almost linear decrease for a few hundred minutes and falling to zero in a more exponential fashion. The *continuous* and the *dashed line* are fits using Eq. 2

period is followed by an almost linear decrease for the next 400–600 min and then starts to deviate from a linear behaviour and leveling to zero slowly in a more or less exponential manner. The fit curves shown are explained below.

The drying time depends on several parameters, like temperature, amount of aerogelic binder, it could depend on the type of sand and its grain size and of course also on the sample length for the fixed diameter.

We first start with the influence of the type and grain size of sand on the drying time, because the result is most astonishing. To determine the influence of the sand properties on the drying process, we dried samples of different sands (length 9 mm, mass 13.5 g) at 40 °C with 10 wt% binder amount. The following sands were used: Cerabeads 400, 650 and 1450, Quartzsand 1 and Sepasil and also Alodur® F80 and F220 (see Table 1). The result is shown in Fig. 3. First of all it is remarkable that all curves look very similar. They have the same shape and seem to be shifted only slightly against each other. Although there are small differences in the time to reach a certain mass loss, these are not that big to be remarkable. The drying in the interstices of the sands seems to be determined by the aerogel only, meaning the chemical composition of the sand, the grain size and thus the permeability of the interstitial network of sand pores seem not to have any appreciable influence.

To determine the relationship between drying time and the amount of binder, we dried samples form Quartzsand 1 (length 27 mm, mass 35 g) with RF-binder amounts of 5, 10, 15 and 20 wt% at 40 °C. The drying times were taken

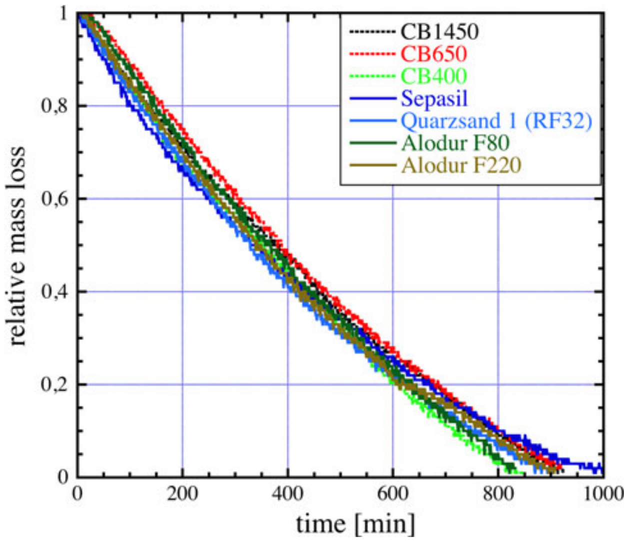

Fig. 3 Drying time of various types of sands having also different grain sizes with 10 wt% RF aerogel as a binder. There are small differences in the time to reach a fixed mass loss, but in general all the curves are very similar and the differences not remarkable

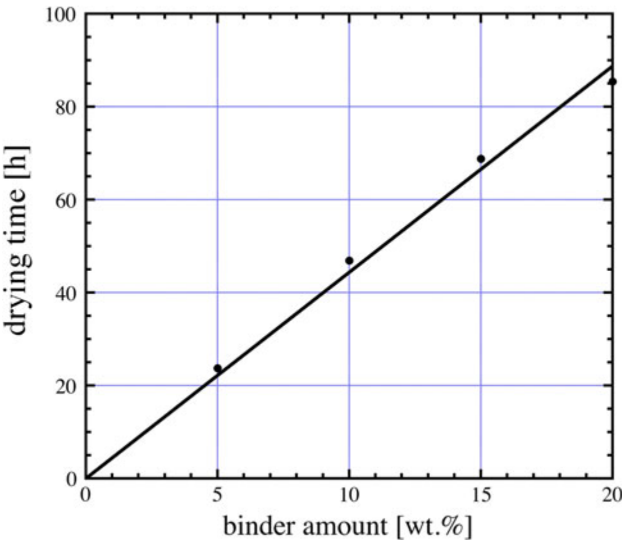

Fig. 4 Drying time of AeroSand samples (Quartzsand 1, sample length 27 mm, sample mass 35 g) in relation to their amount of binder. The drying time grows linear with the binder amount

from figures like those shown in Fig. 2 and defined as that time, when the relative mass loss becomes less than 0.01. The result is shown in Fig. 4 for one temperature. The drying time varies linearly with the binder amount. The line drawn in is a fit forced to go through the origin of the coordinate system.

The dependence on temperature was determined using again Quartzsand 1 (length 27 mm, mass 35 g, binder amount 5 wt%) at temperatures of 20, 40, 50, 60 and 70 °C. The result is shown in Fig. 5. The higher the temperature, the higher the speed of evaporation and the faster

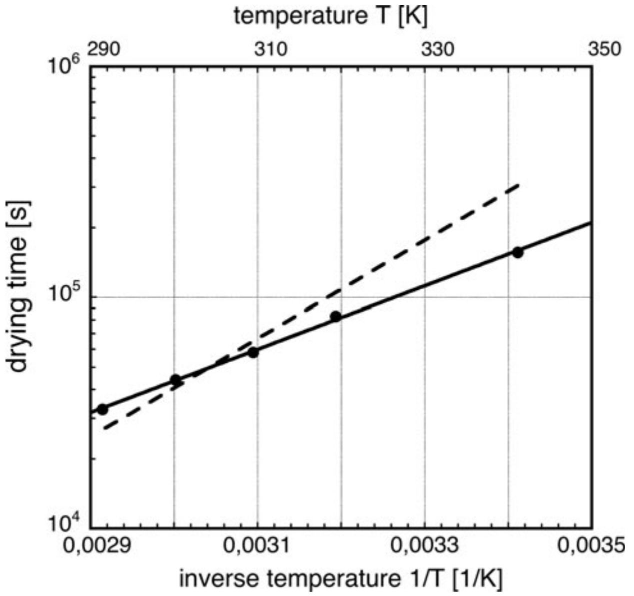

Fig. 5 Drying time of an aerogel-bonded Quartzsand 1 (sample length 27 mm, mass 35 g, binder amount 5 wt%) in relation to the reciprocal drying temperature. The *dotted line* is an exponential fit through the data points. The *dashed line* shows how the drying time would vary if the heat of evaporation of water is used

the drying process. The linear relation between the logarithm of the drying time and inverse temperature suggests an exponential dependence as typical for a thermally activated process.

Evaluating the linear plot in Fig. 5 we obtain for the heat of evaporation an apparent value of $Q_{\mathrm{app}} = 26.2$ kJ/mol. This value might be compared with that of water being 40.7 kJ/mol or that of formaldehyde having a value of 23 kJ/mol. If the solution in the wet gel would be a mixture of both, the solution in the pore network would have during the drying process 20 M fractions water and 80 M fractions formaldehyde (one could also take into account that the formaldehyde used in preparing the RF aerogel solution is stabilized with methanol. Since the heat of vapourization of methanol and water are similar, we omit this distinction). This composition of the evaporating solvent in the sand–aerogel mixture is unrealistic, especially, since during the polycondensation process water is released and methylene bridges are established from the formaldehyde to connect the benzene rings. By this process the polymeric backbone of the RF aerogel particles is built [10, 23]. Therefore, the smaller activation energy value must have a different origin.

The sample length itself has an effect on the drying time. One could expect from a diffusion process a quadratic dependence, since in all diffusive processes a characteristic time always is proportional to a characteristic length squared. A linear relation could be expected, if the process would run with a constant evaporation rate. Then the weight loss is linear in time and should be proportional to the sample length. We therefore varied the sample length and measured again the drying time, using samples of Cerabeads 650 and Alodur F220 with a binder amount: 10 wt%. The result for both sands is shown in Fig. 6. In both cases a linear relation is observed: the longer the sample, the longer is the drying time.

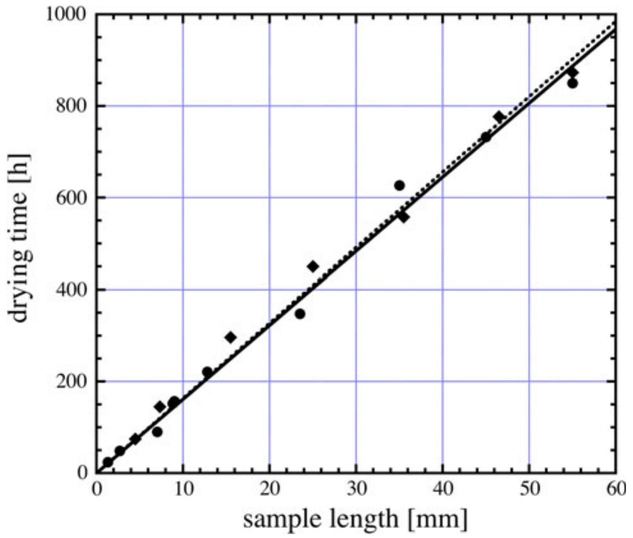

Fig. 6 Drying time for different sample heights for Cerabeads 650 (*full circles*) and Alodur 220 (*full diamonds*). The *lines* are linear fits through the origin. Both *curves* show that the results shown in Fig. 2 are conclusive

The microstructure of a sample was discussed in detail by Reuß and Ratke [5] and Brück and Ratke [2]. For the discussion of the drying process we will only show two examples, to illustrate important aspects of the sand–aerogel structure with respect to drying. Fig. 7a and b shows a fracture surface of a sample with 20 wt% RF aerogel. The whole pore volume of the Alodur sand is filled with the RF aerogel, which exhibits on higher magnification a porous structure well-known from RF aerogels, but considerably smaller in size (particle and pore size) compared to an aerogel of the same chemical composition and prepared with the same processing parameters [10–12]. At lower binder content bonding bridges establish (see Fig. 8a, b), being originally fully liquid (the RF–sol) and become after drying a porous structure as shown in Fig. 7b. The lower binder content also means, that there is, compared with the pore space inside the aerogel, a much larger pore space between the sand grains, with pore size in 10 μm range.

Discussion

The observations shown above can be understood within the context of models describing drying in porous media [16–22] and the microstructure of the aerogel-bonded

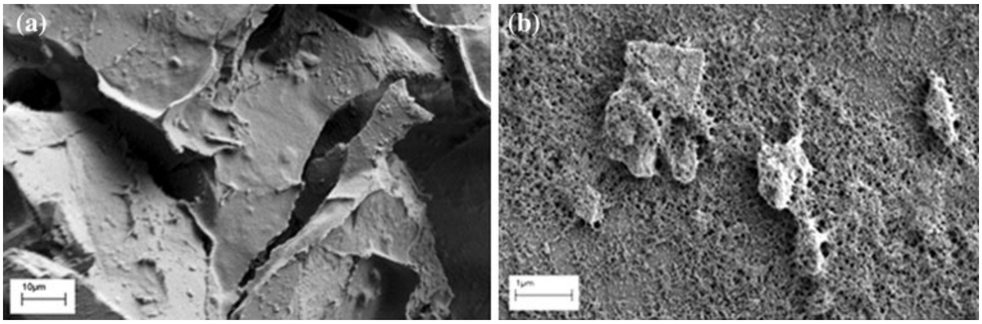

Fig. 7 **a**, **b** Fracture surface of an Alodur sand bonded with 20 wt% RF aerogel. **a** (*left*) shows that the RF aerogel has completely filled the interstitial space between the sand grains. A close-up in **b** (*right*) shows that the aerogel film covering the grains have a fine, submicron scale porous structure

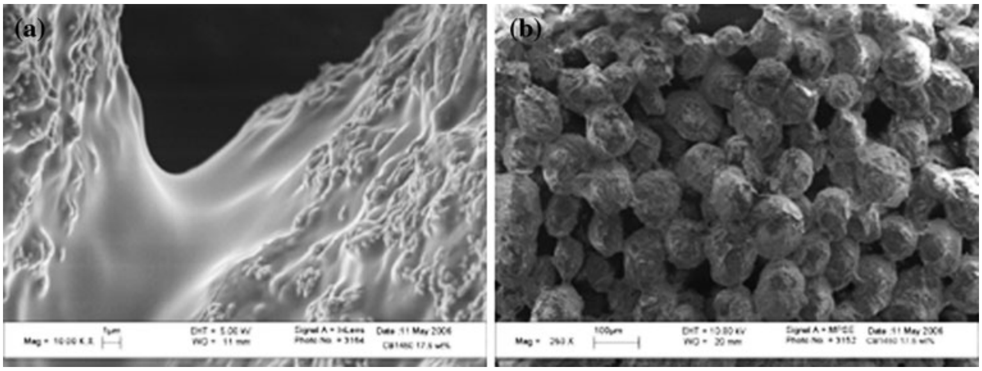

Fig. 8 **a**, **b** Bonding bridge of an RF aerogel between nearly spherical grains of a Cerabead sand (CB1450) with 17.5 wt% RF aerogel dried at room temperature. Besides the bridge it can be seen that the surface of the sand grains is covered by the aerogel. This also is shown in **b** (*right*), revealing that all grains are covered by the aerogel but still enough free interstitial space between the sand grains is left

sands. Essential for the microstructures in all aerogel-bonded sands is that the sand grains are covered with a thin film of the RF aerogel and between them there is a bridge of the aerogel. At higher amounts the whole pore space between the grains is filled with the aerogel. Converting the weight amount of aerogel solution into volume fraction shows, that at 20 wt% the volume fraction is around 43–49% (depending on the density of the sand used). For 5 wt% the volume fraction is already 14–17%. The packing density of the sand was measured by Reuß and Ratke [5, 24] to be typically between 50 and 55 volume percent, i.e., in the range of random-loose packing.

Drying curves of a porous body always can be divided into the regimes shown in Fig. 2 [16, 18, 19]. After an initial period of warming up, the linear fall in weight signals that evaporation of the interstitial liquid dominates. This is due to capillary forces draining the liquid to the surface. When the liquid content becomes smaller such that all liquid–gas interfaces are inside the porous body, diffusion of moisture or humidity or generally the evaporating gases through the porous body determines the weight loss. In the final stage drying depends on the wetting angle between liquid and solid. Hygroscopic materials, like the RF aerogel, will never become really dry, but a certain amount of water might always be left adsorbed.

In the case of aerogel-bonded sands, the situation is somehow more complicated. Initially there is a mixture of sand and RF-solution. This is put into the small furnace shown in Fig. 1. Then directly drying, meaning evaporation of the constituents of the solution occurs, leading to a mass loss. In parallel the formation of colloidal particles and the gelation process start. Since the interstitial space between the sand grains is generally smaller than the sand grains themselves, gelation is much more rapid compared to a sand-free aerogel solution of the same overall size: the critical spanning cluster of the colloidal particles must only reach dimensions of a few ten to hundred micrometres, instead of a few ten millimetres and thus gelation will probably be a factor of 1000 to a million faster in the interstitial space of the sand grains. This means, that the plateau regime shown in Fig. 2 contains the warming up and the building of the gel network. Once this is established, evaporation of the remaining solution occurs via the wet sample surface.

The combination of a nanosized structure inside the sand interstices established by the aerogel and the general models of drying describe why the curves in Figs. 3 and 6 have the same shape and fall almost together. The RF-aerogel binder establishes even at the smallest amount of RF aerogel used, a continuous film, according to theoretical predictions and experimental investigations of water–sand systems by Herminghaus [25] and our observations shown in Fig. 8a and b. This means, that the solution of water, formaldehyde and methanol making the interporous liquid in the aerogels, will be squeezed always to the surface, since the capillary pressure in the aerogel binder with pores of around 50 nm in diameter is much larger than the 50–200 µm pore system in the sand. Therefore, we observe for quite a while an almost linear decrease in weight. After some time, however, diffusion either inside the aerogel (at higher amounts) or inside the porous network of the aerogel-bonded sand becomes more important than the direct evaporation at the surface. Therefore, a linear decrease is always combined with an exponential one. This can be described for instance by a relation like

$$\frac{m(t) - m(\infty)}{m(0) - m(\infty)} = (1 - a_V t)\exp(-b_D t) \tag{2}$$

which fits to the curves in Fig. 2 over a wide range, but not perfectly, especially at longer annealing times.

The data in Fig. 3 instead fit perfectly to such a relation, such that in all fits the a_V and b_D values are within a percent identical. Figure 9 shows an example of drying curves to which the empirical relation fits quite nicely. There are other functions that would equally well fit to the data; we have chosen this one, because the first term reflects the mass loss due to a constant evaporation rate and the second term that due to diffusion in the pore space. Even simple analytical models yield much more complex formulas [21], however, with many unknown parameters.

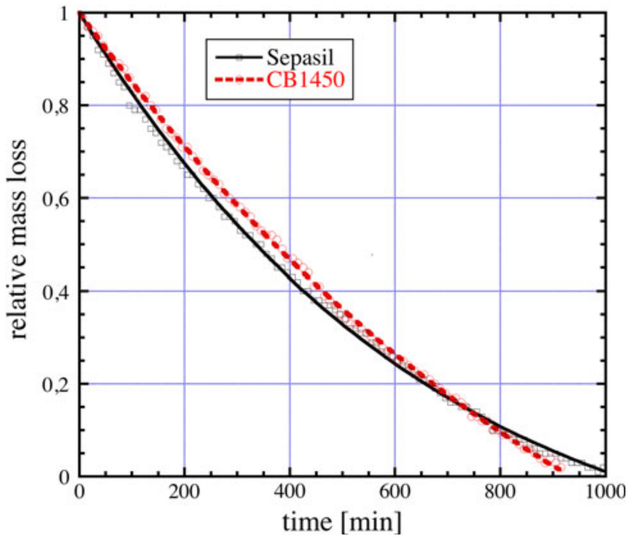

Fig. 9 Drying curves of two sands with 10 wt% RF aerogel (CB1450 and Sepasil) and a drying temperature of 40 °C. Although both *curves* have a different shape, they can nicely be fitted with the simple expression of Eq. 2

The observations presented in Fig. 6 are in agreement with measurements of the drying of porous bodies of clay, gypsum, fired-clay bricks and sand-lime bricks [21]. In these materials a linear progression of the drying front with time into the samples was observed, which can be converted to a linear variation of sample weight with time and thus the final drying time with sample length. Pel and co-authors [21] explain their observation with a moisture dependent diffusion coefficient, for which they assume a functional behaviour allowing them to solve the nonlinear diffusion equation describing moisture transport analytically.

The variation of drying time with binder amount needs no special explanation. This is exactly what is expected: The more liquid binder initially the longer it takes to get rid of it by evaporation. The temperature dependence observed is of the Arrhenius type as expected for a thermally activated process. In Eq. 2 the drying time would be just $1/a_V$. a_V is directly related to the evaporation rate, which can be calculated for instance by simple kinetic gas theory as being proportional directly to the partial pressure. This is exponentially dependent on an activation energy.

The activation energy observed is, however, smaller than expected for a solution consisting mainly of water. If we assume that the capillary tension eases evaporation, one can explain the activation energy. The liquid–gas interface in the pore space of the aerogel is stressed due to capillary forces and therefore the partial pressure is larger compared to a flat interface. This results in a modification of the activation energy, which can be calculated as

$$Q_{\mathrm{app}} = Q_0 - \frac{2V_{\mathrm{m}}\gamma_{\mathrm{LV}}\cos\theta}{\langle r\rangle} \tag{3}$$

in which V_{m} is the molar volume, γ_{LV} the surface tension and $\langle r\rangle$ the average capillary radius, θ the wetting angle between RF aerogel and the solution and Q_0 the activation energy for evaporation above a flat surface. Water has a surface tension of 0.072 J/m^2 at room temperature, that of methanol is about 0.0226 J/m^2 and mixtures of formaldehyde and phenol have values of around 0.070–0.080 J/m^2 [26]. If we take for instance an average pore radius in the aerogel of 100 nm, we easily obtain a reduction in activation energy around 20 kJ/mol. Thus a value of 26 kJ/mol as observed in our samples seems in a range explainable by this simple idea. Note, however, that the absolute value is sensitive to the wetting angle and the pore size distribution within the aerogel binder.

Conclusions

Our experimental results show the drying foundry sands bonded by nanostructured RF aerogels is not influenced by the kind of the sand, its composition, particle shape or the grain size and the porosity. A linear dependence between sample length and drying time was observed and the temperature dependence reveals a thermally activated process. The RF-aerogel binder dominates the drying behaviour in the sense that it constitutes a continuous network of nanopores which drain the liquid to the sample surface establishing an evaporation controlled drying. The capillary stresses reduce the activation energy for evaporation by about 1/3 of its nominal value. The macro-pores in the sand are of minor relevance for the drying process.

Acknowledgement This work was supported by Deutsche Forschungsgemeinschaft (DFG)/Bonn (Ra 537/8).

References

1. Brück S, Ratke L (2003) J Sol–Gel Sci Tech 26:663
2. Brück S, Ratke L (2004) Giesserei Forschung 56:55
3. Brück S, Ratke L (2004) Giesserei 7:22
4. Voss D, Ratke L (2005) Giesserei Forschung 57:18
5. Reuß M, Ratke L (2009) Int Foundry Res 61:24
6. Kistler SS (1932) J Phys Chem 34:S52
7. Hüsing N, Schubert U (1998) Angew Chem Int Ed 37:22
8. Pierre AC, Pajonk GM (2002) Chem Rev 102:S4243
9. Brinker CJ, Scherer GW (1990) Sol–gel–science. Academic Press, New York
10. Pekala RW (1989) J Mater Sci 24:3221. doi:10.1007/BF01139044
11. Fricke J, Emmerling A (1998) J Sol–Gel Sci Technol 13:S299
12. (1995) Proceedings of the 4th internationl symposium on aerogels. J Non-Cryst Solids 186
13. Beeley PR (2001) Foundry technology, 2nd edn. Butterworth-Heinemann, Oxford
14. Campbell J (2000) Castings. Butterworth-Heinemann, Oxford
15. Tilch W, Flemming E (1993) Formstoffe und Formverfahren. Deutscher Verlag für Grundstoffindustrie, Leipzig/Stuttgart
16. Vafai K (2005) Handbook of porous media. CRC Press, Taylor & Francis, Boca Raton
17. Tsotsas E (2003) Magdeburger Wissenschaftsjournal 1–2:63
18. Prat M (2002) Chem Eng J 86:153
19. Vu TH (2006) Influence of pore size distribution on dyring behaviour of porous media by a continuous model. PhD thesis, Otto-von-Guericke University of Magdeburg, Germany
20. Prat M (2007) Int J Heat Mass Transf 50:1455
21. Pel L, Landmann KA, Kaasschieter EF (2002) Int J Heat Mass Transf 45:3173
22. Metzger T, Kwapinski M, Peglow M, Saage G, Tsotsas E (2007) Transp Porous Med 66:103
23. Durairaj J (2005) Resorcinol: chemistry, technology and applications. Springer, Berlin, Heidelberg
24. Reuß M, Ratke L (2010) Int Foundry Res 62:24
25. Herminghaus S (2001) Adv Phys 54:221
26. Hse C-Y (1972) Holzforschung 26:82